JOURNAL OF THEORETICAL AND APPLIED MECHANICS
46, 3, pp. 521-530, Warsaw 2008

QUANTITATIVE ESTIMATION OF THE TOOL WEAR EFFECTS IN A RIPPING HEAD BY RECURRENCE PLOTS

Grzegorz Litak
Technical University of Lublin, Department of Applied Mechanics, Lublin, Poland
e-mail: g.litak@pollub.pl

Jakub Gajewski
Technical University of Lublin, Department of Machine Construction, Lublin, Poland

Arkadiusz Syta
Technical University of Lublin, Department of Applied Mathematics, Lublin, Poland

Józef Jonak
Technical University of Lublin, Department of Machine Construction, Lublin, Poland

We investigate the time series of a torque applied to the ripping head in the process of a cutting concrete rock with sharp and blunt tools. By applying nonlinear embedding methods and the recurrence plots technique to the corresponding time series, we indicate the changes in nonlinear dynamics lying behind the ripping process, and we propose a test of the ripping machine efficiency and a way of monitoring the state of tools.

Key words: ripping head, nonlinear vibrations, recurrence plot

1. Introduction

The dynamics of a cutting process, in the case of metals, was described by Merchant several decades ago (Merchant, 1945). His proposals, involving such phenomena as friction, impacts, and chips breaking, are still inspiring in the current research of metal cutting with higher speeds (Litak, 2002; Sen *et al.*, 2007; Warmiński *et al.*, 2003). They were also extended to the problem of cutting of brittle materials including cutting of rocks. In this paper, we discuss experimental results obtained using the technology of multi-tool ripping heads (Eichbaum, 1980; Fowell, 1993; Gajewski and Jonak, 2006; Jonak and Gajewski, 2008). We will show time histories of the ripping head torque applied to a

standard rock and later examine them by means of embedding and recurrence theories.

The aim of the present paper is to show how recurence plots (RP) and recurence quantification analysis (RQA) can help in the assessment of states of the ripping head tools.

2. Considered problem

Multi-tool ripping torque time histories $T(i)$ versus the sampling index i for sharp and blunt tools are presented in Figs. 1a and 1b, respectively. All other working conditions besides the states of tools were the same. Note, that the times series of sharp tools is characterized by slightly larger peak values. On the other hand, blunt time series shows a characteristic time interval $i \in [3700, 7100]$ of a fairly smaller amplitude, which can indicate on possible intermittency in the examined system.

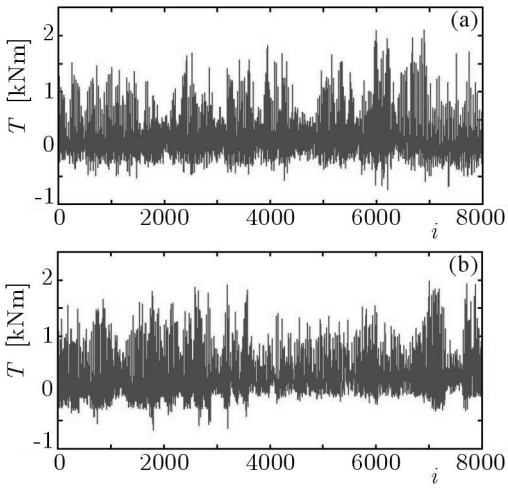

Fig. 1. Multi-tool ripping torque time histories $T(i)$ versus the sampling index i for sharp (a) and blunt (b) tools. The sampling time was 0.005 s while the rotational velocity was 42 rev/min

To go further with the standard methods of nonlinear time series analysis (Fig. 1), one should investigate the embedding properties. This approach is based on properties of a phase space which can be reconstructed by supplementing missing coordinates with time delayed ones (Takens, 1981). Thus, the

examined torque $\boldsymbol{T}_i$ on the ripping head at the sampling time given by i can be expressed as the following vector

$$\boldsymbol{T}_i = [T_i, T_{i-\Delta i}, T_{i-2\Delta i}, \ldots, T_{i-(M-1)\Delta i}] \tag{2.1}$$

where Δi is the time delay in sampling time units, while M is the embedding dimension. Now we explain how to obtain proper values of Δi and M by examining the average mutual information (AMI) (Fraser and Swinney, 1986; Hegger *et al.*, 1999; Kantz and Schreiber, 1997) and the false nearest neighbour fraction (FNNF) (Abarbanel, 1996; Hegger *et al.*, 1999; Kennel and Brown, 1992; Sen *et al.*, 2007). AMI is defined via conditional probabilities of the sequence events

$$\mathrm{AMI}(\delta i) = -\sum_{kl} p_{kl}(\delta i) \ln \frac{p_{kl}(\delta i)}{p_k p_l} \tag{2.2}$$

where, for some partition (16 equal parts) of the ripping head, torque values are in an interval $T \in [T_{min}, T_{max}]$, p_k is the probability of finding a time series value in the k-th interval, and p_{kl} is the joint probability that an observation falls later into the l-th element, and the observation time is given by δi. The optimal time delay $\Delta i = \delta i$ is to be determined by the first AMI minimum for which the examined events are independent enough to define a new coordinate. Note, that AMI is positively defined and its smallest value (theoretically $\mathrm{AMI} = 0$) can be reached when p_{kl} can be factorized to individual probabilities p_k and p_l ($p_{kl} \approx p_k p_l$) for any k and l far from each other by δi.

On the other hand, to get FNNF one has to choose a point indicated by $\boldsymbol{T}_i$ and calculate the distance to its nearest neighbour point $\boldsymbol{T}_j$ in the m-dimensional space. For an Euclidean distance, which is typically used here, it is $|\boldsymbol{T}_i - \boldsymbol{T}_j|_m$.

By iterating both points along the time series, we compute the control parameter $Q_{i,m}$ defined as

$$Q_{i,m} = \frac{|\boldsymbol{T}_i - \boldsymbol{T}_j|_{m+1}}{|\boldsymbol{T}_i - \boldsymbol{T}_j|_m} \tag{2.3}$$

By comparing the above value to a chosen threshold Q_c, we calculate a fraction of cases for which $Q_{i,m}$ exceeds the threshold value Q_c. The FNNF can be then estimated from the following expression

$$\mathrm{FNNF}(m) = \frac{1}{N} \sum_i \Theta(Q_{i,m} - Q_c) \tag{2.4}$$

where N is the number of vector elements in the vector time series, $\Theta(x)$ is the Heaviside step function. This, so called, fraction analysis is repeated by choosing different values of the dimension m. The optimal value $M = m$ is defined when the fraction of false nearest neighbours tends to zero (note, in some cases, depending on Q_c in respect to the standard square deviation of examined time series $T(i)$, some points are omitted and FNNF reaches the minimum for the optimal dimension $m = M$)

$$\lim_{m \to M} \mathrm{FNNF}(m) \to 0 \tag{2.5}$$

3. Results of numerical analysis

Using the above definitions for AMI and FNNF, we have estimated the embedding for the time series of sharp tools. In Figs. 2a,b one can easily find that the optimal values are $\Delta i = 3$ and $M = 7$ representing the time delay and the embedding dimension.

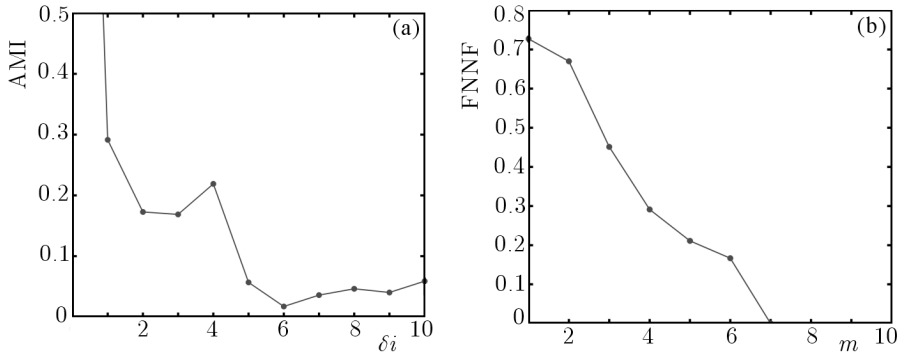

Fig. 2. AMI versus time delay δi (a), FNNF versus embedding dimension m (b) for sharp tools

These results would be a frame for the RP and RQA techniques. Here we assumed that these quantities were slowly evaluating during cutting of rock. To simplify the procedure of monitoring of the tools state, we fixed the embedding in the initial stage (for sharp tools). This can be additionally justified by the existence of important embedding invariants including the Shannon information entropy (Thiel *et al.*, 2004).

The recurrence plot is usually defined by the following matrix form $\mathbf{R}^{m,\epsilon}$ with the corresponding elements $R_{ij}^{m,\epsilon}$ (Casdagli, 1997; Eckmann *et al.*, 1987;

Litak *et al.*, 2007; Marwan, 2003, 2006; Marwan *et al.*, 2007; Thiel etal, 2004; Webber and Zbilut, 1994; Wendeker *et al.*, 2004)

$$R_{ij}^{m,\epsilon} = \Theta(\epsilon - |\boldsymbol{T}_i - \boldsymbol{T}_j|) \tag{3.1}$$

having 0 and 1 elements to be translated into the recurrence plot as an empty place and a black dot, respectively. In this method (RP), patterns showing the diagonal and vertical or horizontal structure of lines are examined. Having obtained such a structure, one can easily classify the dynamics of a studied system (Marwan *et al.*, 2007).

In Fig. 3a and 3b, we mapped the corresponding matrix elements R_{ij} into recurrence plot graphs. One can see that the lines in Fig. 3a are more dense than those in Fig. 3b. As the space between lines corresponds directly to the characteristic period of torque variations, we can conclude that sharp tools variations possess a higher frequency component in their spectrum.

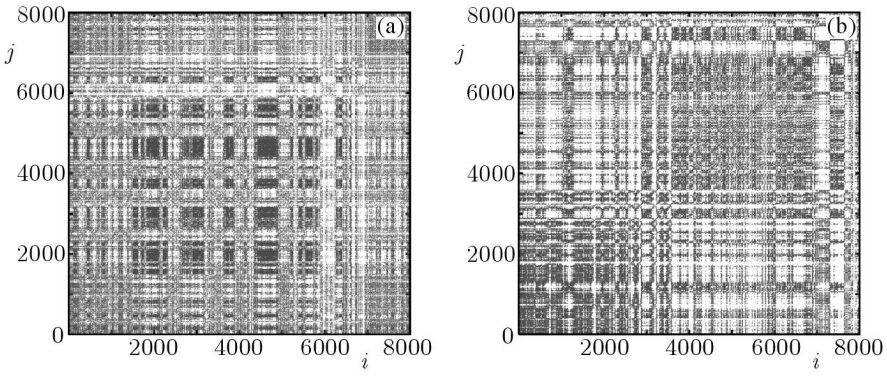

Fig. 3. Recurrence plots for sharp (a) and blunt (b) tools

The other possibility is stronger appearance of random oscillations which usually fill the space between lines uniformly (see the most dense region in the middle of Fig. 3a). On the other hand, a finite length in some of the vertical lines visible in Figs. 3a and 3b invoke the intermittent character of torque changes in both cases (Litak *et al.*, 2007; Marwan *et al.*, 2007; Wendeker *et al.*, 2004).

For quantitative analysis, we define the recurrence rate RR

$$RR = \frac{1}{N^2} \sum_{i,j=1}^{N} R_{ij}^{m,\epsilon} \qquad \text{for} \qquad |i-j| \geqslant w \tag{3.2}$$

which determines the black dots fraction in the RP graph. w denotes the Theiler window used to exclude identical and neighbour points (in our case $w = 1$) from the above summation, Eq. (3.2).

Furthermore, the RQA can be used to identify vertical or diagonal lines through their lengths up to L_{max}, V_{max} for diagonal and vertical lines, respectively. In its frame, the RQA enables one to perform probability $p(l)$ or $p(v)$ distribution analysis of lines according to their lengths l or v (for diagonal and vertical lines). In practice, they are calculated as

$$p(y) = \frac{P^{\epsilon}(y)}{\sum\limits_{y=y_{min}}^{N} P^{\epsilon}(y)} \tag{3.3}$$

where $y = l$ or v, depending on the diagonal or vertical structures in a specific recurrence plot.

For various collections of diagonal and vertical lines with respect to their lengths distributions, Shannon information entropies (L_{entr} and V_{entr}) can be defined via (Marwan, 2003)

$$L_{entr} = -\sum_{l=l_{min}}^{N} p(l)\ln p(l) \qquad V_{entr} = -\sum_{v=v_{min}}^{N} p(v)\ln p(v) \tag{3.4}$$

Other properties of RP as the determinism DET and laminarity LAM as well as the trapping time TT are also based on the probabilities $P^{\epsilon}(x)$

$$DET = \frac{\sum\limits_{l=l_{min}}^{N} lP^{\epsilon}(l)}{\sum\limits_{i,j=1}^{N} R_{i,j}^{m,\epsilon}} \qquad LAM = \frac{\sum\limits_{v=v_{min}}^{N} vP^{\epsilon}(v)}{\sum\limits_{v=1}^{N} vP^{\epsilon}(v)}$$
$$TT = \frac{\sum\limits_{v=v_{min}}^{N} vP^{\epsilon}(v)}{\sum\limits_{v=v_{min}}^{N} P^{\epsilon}(v)} \tag{3.5}$$

In the above equations, l_{min} and v_{min} ($l_{min} = v_{min} = 2$ in our case) denote minimal lengths of the diagonal and vertical lines which should be chosen for a specific dynamical system. The determinism quantity DET is a measure of the predictability of the examined time series and gives the ratio of recurrent points formed in diagonals to all recurrent points. Note that in a periodic system all points would be included in the lines. On the other hand, the laminarity

LAM is a similar measure which corresponds to points formed in vertical lines. For small point-to-point changes (laminar), consecutive points form a vertical line. These measures tell about the dynamics behind sampling point changes, and are strictly connected to the point fraction spanning the diagonal (DET) and vertical (LAM) patterns, respectively. These diagonal and vertical line patterns are skeletons of deterministic features, while any singular point corresponds to randomness in the examined system. Note that for random numbers, the recurence plot is filled uniformly without any pattern. Finally, the trapping time TT refers to the average length of vertical lines measuring the time scale (in terms of sampling intervals) of these small changes in the examined time history.

We performed calculations (using the numerical code provided in Marwan (2006)) of all the specified quantities for our time series (Fig. 1) and included them into Table 1.

Table 1. Summary of recurrence quantification analysis (RQA) for 'sharp' and 'blunt' tools, respectively; $w = 1$ (Theiler,s window), $M = 7$, $\Delta i = 3$ and $l_{min} = 2$, $v_{min} = 2$ recurrence threshold $\epsilon = 4$

Type	RR	DET	LAM	L_{max}	V_{max}	L_{entr}	V_{entr}	TT
'sharp'	0.016	0.341	0.323	72	26	0.811	0.710	2.36
'blunt'	0.025	0.819	0.849	318	43	1.918	1.564	3.30

One can see that for the same threshold value $\epsilon = 4$ (Eq. (3.1)), we have a larger RR for the 'blunt' data. This could be connected with higher correlations of these experimental data. The same effect of correlations is also visible in DET and LAM parameters which tell about the deterministic structure of the data. Note that this structure is much more transparent in the 'blunt' data. On the other hand, the entropies L_{entr} and V_{entr} show that the distribution of length of particular diagonal and vertical lines is complex and broader in the case of the 'blunt' data. Note also the differences in L_{max} and V_{max} (Table 1). These quantities are fairly larger for the 'blunt' data ($L_{max} = 318$ for 'blunt' data while $L_{max} = 72$ for 'sharp' data and $V_{max} = 43$ for 'blunt' data while $V_{max} = 26$ for 'sharp' data) because of the lack of correlations in the 'sharp' data.

4. Concluding remarks

In summary, we carried out recurrence analysis of the dynamical time series of the multi-tool ripping head. By examining the RP results, we found that oscillations in the case of sharp tools have two additional dynamical compo-

nents in the spectrum in the case of blunt tools (Fig. 3a and 3b). The first one is higher frequency, while the second important factor corresponds to random noise.

Comparing the RQA results for both examined cases, one can also notice fundamental differences in the deterministic structure. This structure, expressed by both DET and LAM being close to 1 (see in Table 1 $DET = 0.819$, $LAM = 0.849$), is fairly well defined in the case of blunt tools, while in the case of sharp tools, DET and LAM are much smaller (see in Table 1 $DET = 0.341$, $LAM = 0.323$). This could be an indicator of the effect of wear in tools and used in an automated monitoring procedure of condition of tools.

In a rock cutting process, more attention is paid to the expected size of loosening rock elements, which is strictly connected with energy consumption. For larger pieces, smaller energy is needed. It is obvious that wear in tools directly changing characteristics of friction and impacts could be responsible for different system responses. For instance, the wear effect on the sintered carbides considerably changes their rake angle of the cutting edges. In a consequence for blunt tools, the supplied power increases by about 50% in respect to sharp tools (Jonak and Gajewski, 2008). However, to tell if the recurence plots provide a useful criterion, we need to perform more systematic experiments, especially with different rotational velocities of the ripping head and feed rates. These results will be reported in next publications.

Acknowledgements

This research has been partially supported by the Polish Ministry of Science and Higher Education by Grant No. NN501007033.

References

1. Abarbanel H.D.I., 1996, *Analysis of Observed Chaotic Data*, Springer, Berlin
2. Casdagli M.C., 1997, Recurrence plots revisited, *Physica D*, **108**, 12-44
3. Eckmann J.-P., Kamphorst S.O., Ruelle D., 1987, Recurrence plots of dynamical systems, *Europhys. Lett.*, **5**, 973-977
4. Eichbaum F., 1980, *Schneidend-brechende Gewinnung mit der Schneidscheibe. Experimentell und theoretische Untersuchungen*, Gluckauf-Betriebsbucher, Band 22, Verlag Gluckauf GMBH Essen
5. Fowell R.J., 1993, The mechanics of rock cutting, *Comprehensive Rock Engineering*, **4**, 155-175

6. Fraser A.M., Swinney H.L., 1986, Independent coordinates for strange attractors from mutual information, *Phys. Rev. A*, **33**, 1134-1140

7. Gajewski J., Jonak J., 2006, Utilisation of neural networks to identify the status of the cutting tool point, *Tunnelling and Underground Space Technology*, **21**, 180-184

8. Hegger R., Kantz H., Schreiber T., 1999, Practical implementation of nonlinear time series methods: The TISEAN package, *Chaos*, **9**, 413-435

9. Jonak J., Gajewski J., 2008, Identification of ripping tool types with the use of characteristic statistical parameters of time graphs, *Tunnelling and Underground Space Technology*, **23**, 18-24

10. Kantz H., Schreiber T., 1997, *Non-linear Time Series Analysis*, Cambridge University Press, Cambridge

11. Kennel M.B., Brown R., Abarbanel H.D.I., 1992, Determining embedding dimension for phase-space reconstruction using a geometrical construction, *Physical Review A*, **45**, 3403-3411

12. Litak G., 2002, Chaotic vibrations in a regenerative cutting process, *Chaos, Solitons and Fractals*, **13**, 1531-1535

13. Litak G., Kamiński T., Czarnigowski J., Żukowski D., Wendeker M., 2007, Cycle-to-cycle oscillations of heat release in a spark ignition engine, *Meccanica*, **42**, 423-433

14. Marwan N., 2003, *Encounters with Neighbours: Current Development of Concepts Based on Recurrence Plots and their Applications*, PhD Thesis, Universität Potsdam, Potsdam

15. Marwan N., 2006, *Recurrence Plots Code*, http://www.agnld.uni-potsdam.de/∼marwan/6.download/rp.php

16. Marwan N., Romano M.C., Thiel M., Kurths J., 2007, Recurrence plots for the analysis of complex systems, *Physics Reports*, **438**, 237-329

17. Merchant E.M., 1945, Mechanics of the metal cutting process, *J. Appl. Phys.*, **11**, 267-275

18. Sen A.K., Litak G., Syta A., 2007, Cutting process dynamics by nonlinear time series and wavelet analysis, *Chaos*, **17**, 2797-2803

19. Takens F., 1981, *Detecting Strange Attractors in Turbulence*, Lecture Notes in Mathematics, **898**, Springer, Heidelberg, 366-381

20. Thiel M., Romano M.C., Read P.L., Kurths J., 2004, Estimation of dynamical invariants without embedding by recurrence plots, *Chaos*, **14**, 234-243

21. Warmiński J., Litak G., Cartmell M.P., Khanin R., Wiercigroch M., 2003, Approximate analytical solutions for primary chatter in the nonlinear metal cutting model, *Journal of Sound and Vibration*, **259**, 917-933

22. Webber C.L. Jr., Zbilut J.P., 1994, Dynamical assessment of physiological systems and states using recurrence plot strategies, *J. App. Physiol.*, **76**, 965-973

23. Wendeker M., Litak G., Czarnigowski J., Szabelski K., 2004, Nonperiodic oscillations of pressure in a spark ignition combustion engine, *Int. J. Bif. and Chaos*, **14**, 1801-1806

Szacowanie ilościowe wpływu stępienia narzędzia na pracę głowicy urabiającej za pomocą wykresów rekurencyjnych

Streszczenie

W artykule przedstawiono wyniki badań nad zastosowaniem nieliniowych metod zanurzenia oraz wykresów rekurencyjnych do oceny zmian dynamicznych zachodzących w procesie urabiania. Przebadano przebiegi czasowe momentu urabiania głowicą uzbrojoną w ostre oraz stępione narzędzia górnicze. Proponowane metody mogą okazać się przydatne w kontekście oceny wydajności oraz monitorowania stanu narzędzi głowicy urabiającej.

Manuscript received November 11, 2007; accepted for print March 28, 2008